THE JOURNAL OF BIOLOGICAL CHEMISTRY VOL. 286, NO. 3, pp. 2320–2330, January 21, 2011

The MARCKS Protein Plays a Critical Role in Phosphatidylinositol 4,5-Bisphosphate Metabolism and Directed Cell Movement in Vascular Endothelial Cells*[S]

Received for publication, October 19, 2010, and in revised form, November 16, 2010 Published, JBC Papers in Press, November 20, 2010, DOI 10.1074/jbc.M110.196022

Hermann Kalwa and Thomas Michel[1]

From the Cardiovascular Medicine Division, Department of Medicine, Brigham and Women's Hospital, Harvard Medical School, Boston, Massachusetts 02115

The MARCKS protein (myristoylated alanine-rich C kinase substrate) is an actin- and calmodulin-binding protein that is expressed in many mammalian tissues. The role of MARCKS in endothelial signaling responses is incompletely understood. We found that siRNA-mediated knockdown of MARCKS in cultured endothelial cells abrogated directed cell movement in a wound healing assay. We used biochemical and cell imaging approaches to explore the role of MARCKS in endothelial signal transduction pathways activated by insulin. Insulin treatment of vascular endothelial cells promoted the dose- and time-dependent phosphorylation of MARCKS. Cell imaging and hydrodynamic approaches revealed that MARCKS is targeted to plasmalemmal caveolae and undergoes subcellular translocation in response to insulin. Insulin treatment promoted an increase in levels of the signaling phospholipid phosphatidylinositol 4,5-bisphosphate (PIP_2) in plasmalemmal caveolae. The insulin-stimulated increase in caveolar PIP_2 was blocked by siRNA-mediated knockdown of MARCKS, as determined using both biochemical assays and imaging studies using FRET-based PIP_2 biosensors. The critical role of PIP_2 in MARCKS responses was explored by examining the PIP_2- and actin-binding proteins Arp2/3 and N-WASP. Insulin promoted the rapid and robust phosphorylation of both N-WASP and Arp2/3, but these phosphorylation responses were markedly attenuated by siRNA-mediated MARCKS knockdown. Moreover, MARCKS knockdown effectively abrogated N-WASP activation in response to insulin, as determined using a FRET-based N-WASP activity biosensor. Taken together, these studies show that MARCKS plays a key role in insulin-dependent endothelial signaling to PIP_2 and is a critical determinant of actin assembly and directed cell movement in the vascular endothelium.

The MARCKS protein (myristoylated alanine-rich C kinase substrate) was discovered in 1989 as a phosphoprotein abundantly expressed in neuronal tissues. Over the years, MARCKS has been shown to bind reversibly to a broad spectrum of important structural and regulatory molecules, including actin, Ca^{2+}/calmodulin, and the signaling phospholipid phosphatidylinositol 4,5-bisphosphate (PIP_2)[2] (1). Phosphorylation of MARCKS leads to its intracellular translocation, associated with a decrease in calmodulin and PIP_2 binding; MARCKS phosphorylation also promotes its interactions with actin and actin-binding proteins. The actin-binding properties of MARCKS have been implicated in control of cell adhesion and motility (2), yet much less is known about the receptor-modulated pathways that control MARCKS phosphorylation. The MARCKS-null mouse is embryonic lethal because of severe neural defects (3), yet no tissue-specific MARCKS knockout mouse models have been reported. Whereas the presence of the MARCKS protein has been documented in a wide variety of cells and tissues, there are major gaps in our understanding of the roles of MARCKS in receptor-modulated signaling pathways. Our studies focused on analyzing the roles of MARCKS in vascular endothelial cells, a cell type notable for its remarkable diversity of interconnected signaling pathways, many of which are targeted to plasmalemmal caveolae.

In endothelial cells, plasmalemmal caveolae serve as sites for the sequestration of diverse receptors, G-proteins, protein and lipid kinases and phosphatases, and many other signaling molecules. Plasmalemmal caveolae are also characterized by having a distinct lipid composition and are enriched in PIP_2 and other signaling lipids (4). Many caveola-targeted signaling pathways are modulated by the scaffolding/regulatory protein caveolin-1, which is an important constituent of plasmalemmal caveolae. Like MARCKS, caveolin-1 also binds to specific lipids and to actin (5–7). Although the pathways that regulate MARCKS targeting to caveolae are largely unknown, the interactions between MARCKS with membrane phospholipids have been explored extensively (8–10). When MARCKS is phosphorylated, its binding affinity to membrane phospholipids is decreased, and MARCKS may be released from the plasma membrane and translocate to perinuclear regions of the cell (8–10). MARCKS phosphorylation and translocation are associated with alterations in the actin cytoskeleton (11) and may lead to changes in cell motility (2).

* This work was supported, in whole or in part, by National Institutes of Health Grants GM36259, HL48743, and HL46457 (to T. M.). This work was also supported by Postdoctoral Fellowship PDR-09-002 from the Fonds National de la Recherche (Luxembourg) (to H. K.).

[S] The on-line version of this article (available at http://www.jbc.org) contains supplemental Figs. 1 and 2.

[1] To whom correspondence may be addressed: 75 Francis St., Thorn Bldg. 1210A, Boston, MA 02115. Tel.: 617-732-7376; Fax: 617-732-5132; E-mail: thomas_michel@harvard.edu.

[2] The abbreviations used are: PIP_2, phosphatidylinositol 4,5-bisphosphate; BAEC, bovine aortic endothelial cells; PLC, phospholipase C; PH, pleckstrin homology.

MARCKS thus has the distinctive characteristics of binding both to the phospholipid PIP_2 as well as to actin. The PIP_2-binding WAVE proteins represent one of the few other protein families that share this feature of binding both to membrane phospholipids and to the actin cytoskeleton. The PIP_2-binding WAVE family member N-WASP and its downstream actin-binding protein Arp2/3 (12–14) represent attractive candidates for partnering with MARCKS in intracellular signaling. However, the interactions of MARCKS, WAVE proteins, and Arp2/3 in control of endothelial signaling pathways are almost entirely unexplored.

As implied by its name, MARCKS is a target for phosphorylation by PKC. In adipocytes, insulin-stimulated PKC activation leads to MARCKS phosphorylation (15). In vascular endothelial cells, insulin treatment leads to the activation of several PKC isoforms as well as kinase Akt (16). Insulin-dependent endothelial signaling pathways are aberrant in diabetes and other vascular disease states (17). In addition to its well characterized roles in muscle, fat, and liver, insulin is emerging as a critical determinant of vascular function (17). However, the role of insulin in regulation of MARCKS-modulated responses in endothelial cells is largely unexplored.

These studies examined the role of MARCKS in insulin-activated signaling pathways in vascular endothelial cells. We used RNA interference methods, biochemical approaches, and novel biosensors to explore the effects of siRNA-mediated MARCKS knockdown on PIP_2 metabolism and PIP_2-modulated signaling responses involving the PIP_2-binding WAVE protein N-WASP and its actin-binding partner Arp2/3. These studies revealed novel connections between phospholipids and the actin cytoskeleton that are regulated by MARCKS and critically influence directed cell movement in the vascular endothelium.

EXPERIMENTAL PROCEDURES

Materials and Methods—FBS was purchased from HyClone Laboratories. All other cell culture reagents, media, and Lipofectamine 2000 were from Invitrogen. FuGENE 6 transfection reagent was from Roche Applied Science. LY294002, phorbol 12-myristate 13-acetate, and calphostin C were from Calbiochem. Antibodies directed against Akt, phospho-Akt (Ser-473), pan-phospho-PKC, phospho-ERK1/2 (Thr-202/Tyr-204), and ERK1/2 were from Cell Signaling Technology, Inc. Polyclonal antibodies against phospho-N-WASP (Thr-237), phospho-N-WASP (Ser-484/Ser-485), N-WASP, phospho-Arp2/3 (Ser-265), and Arp2/3 were from ECM Biosciences (18, 19). Total and phospho-MARCKS antibodies were from CellTec. Polyclonal antibody against caveolin-1 was from BD Transduction Laboratories. The GST-PLCδ1PH fusion proteins were from Echelon Bioscience. Alexa Fluor 488- and Alexa Fluor 568-coupled secondary antibodies and phalloidin/Alexa Fluor 568 were from Invitrogen. SuperSignal chemiluminescence detection reagents and secondary antibodies conjugated with HRP were from Pierce. The FRET biosensor plasmids PLCδ1PH-YFP and PLCδ1PH-CFP for PIP_2 detection were the kind gift of Professor Kees Jalink (National Cancer Institute, Amsterdam, The Netherlands) (20). The N-WASP-BS FRET biosensor for N-WASP was the kind gift of Professor John Condeelis (Albert Einstein College of Medicine) (21). All other reagents were from Sigma.

siRNA Design—On the basis of established characteristics of siRNA-targeting constructs (22, 23), we designed a MARCKS duplex siRNA corresponding to bases 223–241 from the open reading frame of the bovine MARCKS mRNA: 5′-GCG CUU UUC CUU CAA GAA-dTdT-3′. The RNA sequence used as a negative control for siRNA activity was 5′-GCG CGC UUU GUA GGA UUC G-dTdT-3′. All duplex siRNA-targeting constructs were purchased from Ambion.

Cell Culture and Transfection—Bovine aortic endothelial cells (BAEC) were obtained from Genlantis (San Diego, CA) and maintained in culture in Dulbecco's modified Eagle's medium supplemented with fetal bovine serum (10%, v/v) as described previously (24). Cells were plated onto gelatin-coated culture dishes and studied prior to cell confluence between passages 6 and 8. siRNA transfections were performed as described previously (25). Briefly, 24 h after cells were split at a 1:8 ratio, and duplex siRNA constructs (final concentration 30 nM) were transfected using Lipofectamine 2000 (0.15%, v/v), following the protocol provided by the manufacturer. Lipofectamine 2000 was then removed by changing into fresh medium containing 10% FBS 5 h after transfection. Plasmid transfection was carried out with FuGENE 6 at a ratio of 1:3 (w/v) according to the manufacturer's protocol. For combined transfections of siRNA-targeting constructs plus plasmid cDNA, the siRNA was transfected first as described above. 5 h after siRNA transfection, the medium was replaced, and the DNA mixture in FuGENE 6 was added and incubated with the cells overnight, at which point the medium was replaced again. Cells were analyzed for a total of 48 h following siRNA transfections.

Scratch Wound Cell Migration Assay—Cell migration was assayed using BAEC. Cells were transfected with siRNA-targeting constructs as described above, and scratch wound experiments were performed 48 h after transfection. 18 h prior to performing the assay, the medium was changed, and cells were starved in Dulbecco's modified Eagle's medium supplemented with 0.4% FBS. Cells were then trypsinized and counted; 2×10^5 cells in Dulbecco's modified Eagle's medium with 0.4% FBS were then added to each chamber in an 8-well cell culture chamber (IBIDI, Munich, Germany) to obtain a continuous monolayer and allowed to adhere for 24 h. After applying a linear scratch in the cell monolayer using a sterile pipette tip, the chamber was mounted onto an inverted Olympus DSU microscope with a stage incubator, and the chamber was monitored continuously for 12 h, with an image taken every 5 min. The imaging was performed in differential interference contrast mode with a ×10 objective.

Cell Treatments and Immunoblot Analyses—Insulin was solubilized in water and stored at −20 °C. LY294002, phorbol 12-myristate 13-acetate, and calphostin C were dissolved in dimethyl sulfoxide and stored at −20 °C. After drug treatments, lysates from BAEC were prepared using a cell lysis buffer (50 mM Tris-HCl (pH 7.4), 150 mM NaCl, 1% Nonidet P-40, 0.025% sodium deoxycholate, 1 mM EDTA, 2 mM Na_3VO_4, 1 mM NaF, 2 μg/ml leupeptin, 2 μg/ml antipain, 2 μg/ml soybean trypsin inhibitor, 2 μg/ml lima trypsin inhibi-

tor). Immunoblot analyses of protein expression and phosphorylation were performed as described previously (25). Detection and quantitation of immunoblots were performed using a ChemiImager HD4000 (AlphaInnotech, San Leandro, CA).

Hydrodynamic Analyses of Caveolar PIP_2 Content—Caveolae-enriched lipid raft fractions were separated by ultracentrifugation in a discontinuous sucrose gradient system as reported previously (26). In brief, transfected BAEC from 100-mm dishes were harvested into 2 ml of buffer containing 500 mM sodium carbonate (pH 11). The lysates were homogenized (40 strokes in a Dounce homogenizer) and sonicated (three 20-s bursts in a Branson Sonifier 450). The resulting cell suspension was brought to 45% sucrose by adding 2 ml of 90% sucrose prepared in MES-buffered saline (25 mM MES (pH 6.5) and 150 mM NaCl) and placed at the bottom of a 12-ml ultracentrifuge tube. A discontinuous gradient was formed above the 45% sucrose bed by adding 4 ml each of 35 and 5% sucrose solutions (prepared in MES-buffered saline containing 250 mM sodium carbonate) and centrifuging at 39,000 rpm for 16–20 h in a TH-641 rotor (Sorvall, Asheville, NC). Twelve 1-ml fractions were collected, starting at the top of each gradient, and an equal volume of each fraction was analyzed by slot blot immunodetection as described above for immunoblot analyses. Fractions were probed with antibodies directed against MARCKS, caveolin-1, or PIP_2-specific GST-PLCδ1PH fusion proteins (27, 28).

Confocal Fluorescence Microscopy—BAEC grown on glass-bottomed dishes (Mattek, Boston, MA) or on glass coverslips were treated as indicated, fixed with 4% paraformaldehyde in PBS for 10 min, rinsed with PBS, permeabilized in 0.1% Triton X-100 in PBS for 5 min, and blocked with 10% goat serum in PBS for 1 h. Incubations with primary antibodies were performed in blocking solution for 1 h at room temperature. After washing with PBS, cells were incubated with appropriate secondary antibodies conjugated to immunofluorescent dyes (Alexa Fluor 488 anti-mouse IgG or Alexa Fluor 568 anti-rabbit IgG) in blocking solution for 1 h at room temperature. After washing three times with PBS, coverslips were mounted on slides using a medium containing 4′,6-diamidino-2-phenylindole as nuclear counter stain. Microscopic analysis of samples was performed using an Olympus IX81 inverted microscope in conjunction with a DSU spinning disk confocal system equipped with a Hamamatsu Orca ER cooled CCD camera. Images were acquired using a ×60 differential interference contrast oil immersion objective lens and analyzed using MetaMorph software (Universal Imaging, Downingtown, PA).

F-actin Visualization—F-actin was stained with phalloidin/Alexa Fluor 568. Cells were fixed and permeabilized as described above and then incubated with phalloidin/Alexa Fluor 568 (100 nM) for 30 min. Microscopic analysis of samples was performed using an Olympus DSU spinning disk confocal system. Images were acquired using a ×60 or ×100 differential interference contrast oil immersion objective lens and analyzed using MetaMorph.

Determination of MARCKS-mediated PIP_2 Release by FRET—All live-cell FRET imaging experiments were carried out in HEPES-buffered saline (140 mM NaCl, 6 mM KCl, 1.25 mM $MgCl_2$, 2 mM $CaCl_2$, 10 mM HEPES, and 5 mM glucose (pH 7.4)). Monitoring of PIP_2 dynamics using FRET has been described in detail previously (20). In brief, BAEC were transiently transfected with PLCδ1PH-YFP and PLCδ1PH-CFP plasmids (gift of Professor Kees Jalink) at a 1:1 ratio. When bound to PIP_2 at the membrane, these intermolecular biosensor constructs are in close proximity and exhibit FRET (19). Excitation of CFP-PH was at 425 ± 10 nm, and emission was collected at 475 ± 10 (CFP) and 540 ± 10 nm (YFP) using the Semrock FRET-CFP/YFP-B four-filter, single-band set. A series of fluorescence images were taken at 30-s time intervals; visualization and analysis were performed using the MetaMorph FRET module. FRET was expressed as ratio of CFP to YFP signals, and changes were expressed as normalized deviation from the initial value.

Determination of MARCKS-mediated N-WASP Activation by FRET—Monitoring of N-WASP activation by FRET was performed using methods described in detail previously (21). In brief, BAEC were transiently transfected with a plasmid encoding the N-WASP FRET biosensor (gift of Professor John Condeelis) (21). Upon activation, this molecular construct undergoes a structural change that leads to a decrease in FRET ratio. Excitation of CFP-PH was at 425 ± 10 nm, and emission was collected at 475 ± 10 (CFP) and 540 ± 10 nm (YFP) using the Semrock FRET-CFP/YFP-B four-filter, single-band set. A series of fluorescence images were taken at 30-s time intervals; visualization and analysis were performed using the MetaMorph FRET module.

Other Methods—All experiments were performed at least three times. Mean values for experiments were expressed as mean ± S.E. Statistical differences were assessed by analysis of variance. A p value <0.05 was considered statistically significant.

RESULTS

To establish the role of MARCKS in the regulation of endothelial cellular responses, we explored the effects of siRNA-mediated MARCKS knockdown on directional migration in an endothelial wound healing assay. This assay has been extensively validated (29) and consists of inducing a "wound" in a confluent monolayer of cultured endothelial cells (typically using a razor blade or pipette tip) and then determining the rate and extent of endothelial cell migration into the denuded area by time-lapse video microscopy. Fig. 1 shows the results of the wound healing assay analyzed in cultured endothelial cells that had been transfected either with control siRNA or with a MARCKS-specific duplex siRNA-targeting construct. As shown, siRNA-mediated MARCKS knockdown markedly attenuated endothelial wound healing. Fig. 1*A* shows selected time-lapse photomicrographs taken after inducing the wound, and Fig. 1*B* shows the quantitative analysis of pooled data. The striking difference in endothelial wound healing as a consequence of siRNA-mediated MARCKS knockdown is highly significant ($p < 0.001$, $n = 3$). siRNA-mediated MARCKS knockdown also blocked the VEGF-promoted increase in wound healing (Fig. 1*C*). The duplex siRNA MARCKS targeting construct resulted in efficient (~90%) and specific MARCKS knock-

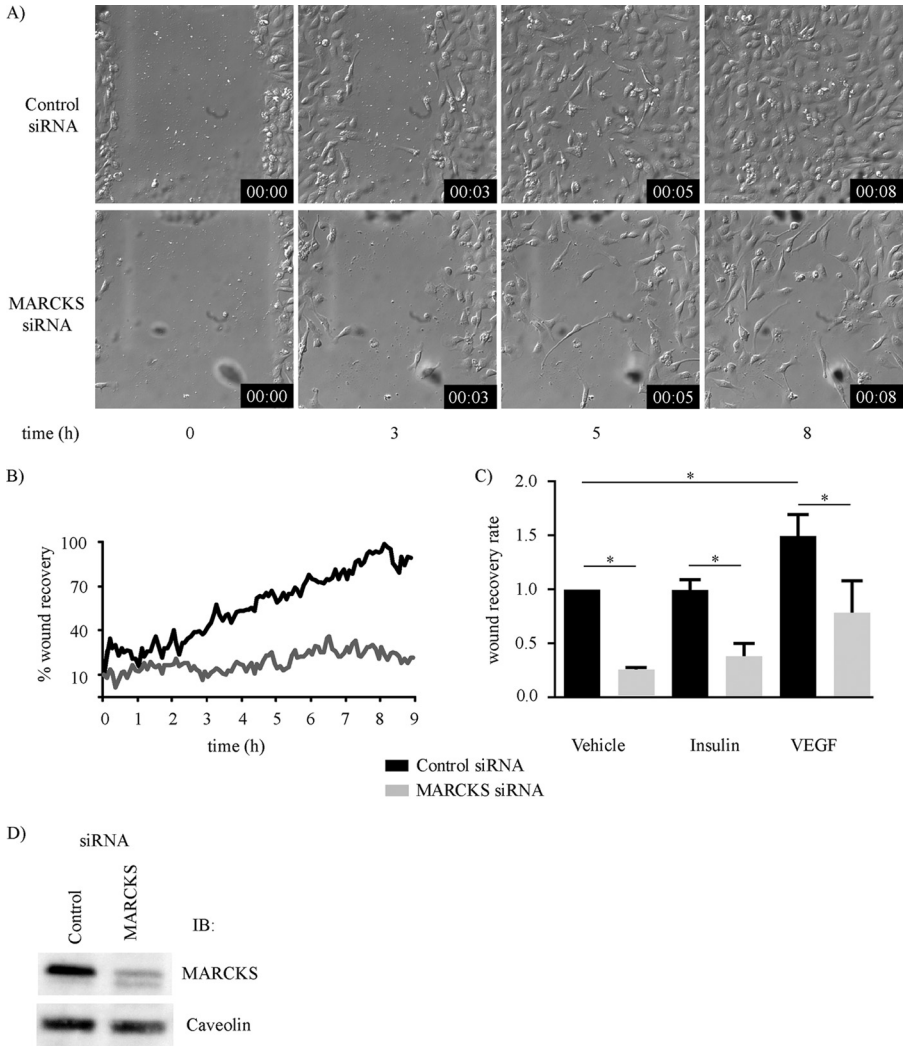

FIGURE 1. **Effects of siRNA-mediated MARCKS knockdown on endothelial cell wound healing.** Shown are the results of a wound healing assay analyzed in cultured endothelial cells transfected 48 h previously with either control or MARCKS duplex siRNA constructs. *A*, selected time-lapse photomicrographs (magnification ×10) obtained at the indicated times after producing a linear wound in the endothelial monolayer; the borders of the wound at t = 0 are noted. Differential interference contrast images were recorded every minute for 8 h using live-cell imaging conditions in an Olympus DSU microscope; the experiment shown was repeated three times with equivalent results. *B*, pooled data from three independent experiments in which the percentage of the original wound that is occupied by cells is plotted as a function of time, and then quantitated using Image J software. The difference in the rate of wound recovery is highly significant between the control and MARCKS siRNA-transfected endothelial cells ($p < 0.001$, $n = 3$). *C*, the results of wound healing assays analyzed after transfection of endothelial cells with control or MARCKS siRNA. They were then studied following cell wounding in the presence of the vehicles, VEGF (20 ng/ml), and insulin (100 nM), as shown. The fractional repopulation of the wound by endothelial cells is shown on the ordinate, as in *B*. *D*, an immunoblot of endothelial cells transfected with control or MARCKS siRNA-targeting constructs, and probed with antibodies as shown.

down (Fig. 1*D* and subsequent figures). We further validated the MARCKS siRNA-targeting construct by exploring the effects of this siRNA on the abundance of numerous endothelial signaling and found no effect on the abundance of any of these proteins (supplemental Fig. 1). We also designed and validated a second independent MARCKS siRNA-targeting construct and found that this construct had the same effect on suppressing directed endothelial cell migration, whereas it had no effect on the abundance of a broad panel of signaling proteins (supplemental Fig. 1).

With the importance of MARCKS in control of a key endothelial cell response established by these observations on directed cell migration, we next turned to a more detailed series of studies of the intracellular signaling pathways modulated by MARCKS. Because many MARCKS responses are mediated by phosphorylation (15, 30, 31), we explored the effects of insulin, which has been extensively shown to activate many protein kinases, including protein kinase C, in endothelial cells (15, 32). Indeed, we found that insulin treatment as well as phorbol ester markedly increased MARCKS phosphorylation in endothelial cells (supplemental Fig. 2). Insulin also led to the phosphorylation of several well known insulin-responsive protein kinases, including protein kinase C, kinase Akt, and ERK1/2; these responses were blocked by the protein kinase C inhibitor calphostin and by the PI3K inhibitor LY294002 (supplemental Fig. 2). Fig. 2 presents a more detailed characterization of the dose-response (*A*) and time course (*D*) for insulin-promoted MARCKS phosphorylation, showing that insulin treatment markedly increases the phosphorylation of MARCKS and kinase Akt in a dose- and time-dependent manner. Fig. 2 (*A* and *D*) shows representative immunoblots, and the panels below show quantitative analyses

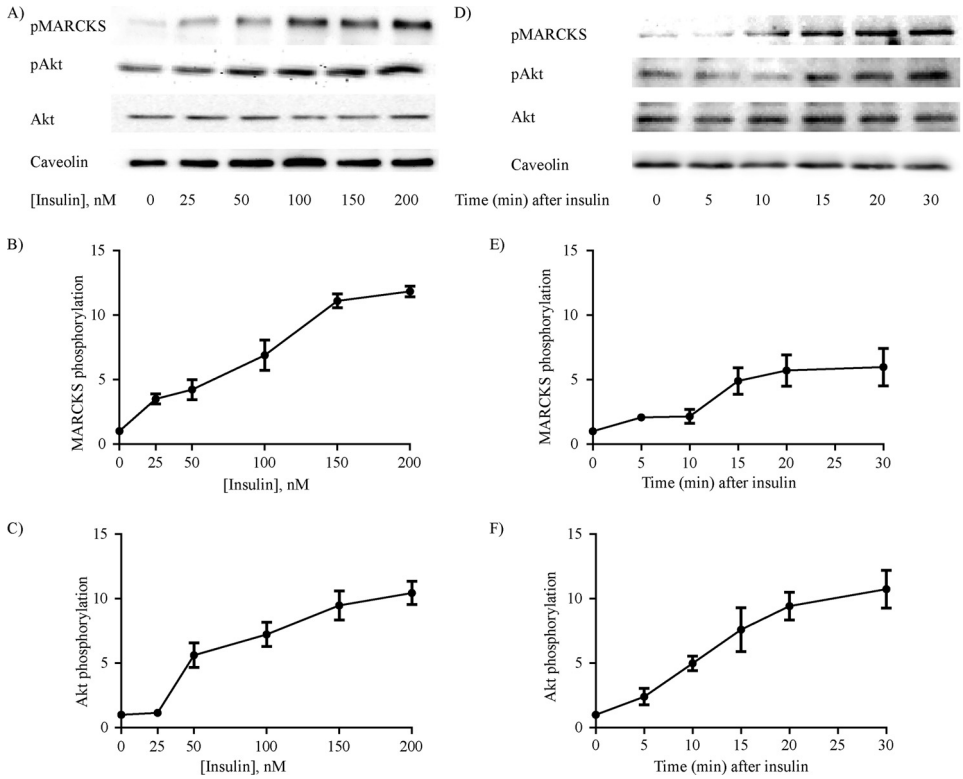

FIGURE 2. **Insulin-stimulated MARCKS phosphorylation in endothelial cells.** Shown here are the results of dose response (*A–C*) and time course (*D–F*) experiments exploring insulin-mediated MARCKS phosphorylation responses in endothelial cells. Lysates prepared from insulin-treated endothelial cells were resolved by SDS-PAGE and analyzed in immunoblots probed with antibodies as shown against total or phosphorylated MARCKS (*pMARCKS*), or antibodies directed against total or phosphorylated Akt (*pAkt*). In the time course experiments, cells were treated with 100 nM insulin; in the dose response experiments, cells were analyzed 15 min after addition of insulin. *A* and *D*, representative immunoblots; *B* and *C*, and *E* and *F* present quantitative plots derived from pooled data; each point in the graphs represents the mean ± S.E. of four independent experiments that yielded similar results.

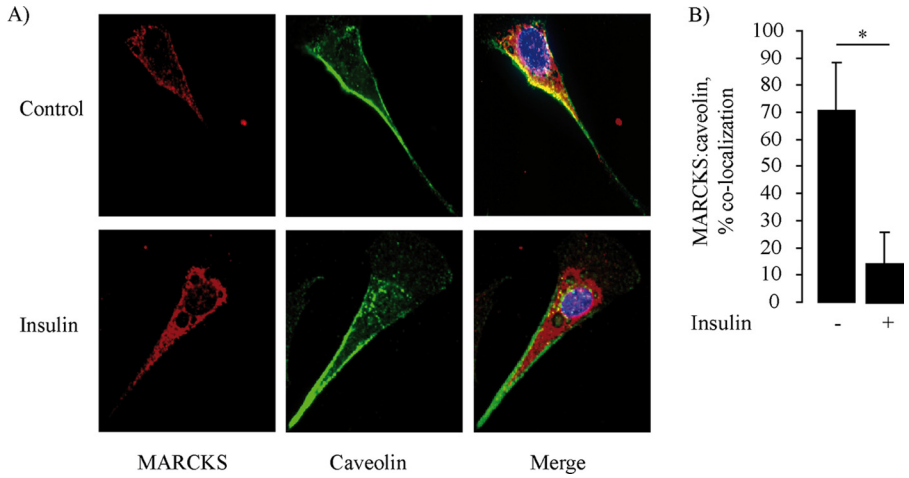

FIGURE 3. **Insulin-stimulated translocation of MARCKS in cultured endothelial cells.** Shown are representative photomicrographs of endothelial cells treated with insulin (100 nM) or vehicle, fixed, and then stained with antibodies directed against MARCKS or caveolin-1. Detection was carried out with secondary antibodies coupled to Alexa Fluor 488 or Alexa Fluor 568, respectively. Nuclei were stained with 4′,6-diamidino-2-phenylindole. *A*, representative images of the staining pattern obtained for MARCKS and caveolin antibodies, analyzed in two-dimensional projections of three-dimensional optical stacks that where obtained by white light confocal imaging (magnification ×60). The MARCKS staining pattern is shown in *red*; caveolin in *green*; and colocalization in *yellow*. *B*, statistical analyses obtained using the MetaMorph colocalization analysis module. Each *bar* represents the mean ± S.E. of five independent experiments that yielded similar results. *, $p < 0.05$.

of pooled data. The EC_{50} for insulin-stimulated MARCKS or Akt phosphorylation is ~100 nM; within 10 min following insulin addition, MARCKS and Akt phosphorylation increased significantly and remained elevated for at least 30 min.

Because the phosphorylation of MARCKS has been associated with its intracellular translocation (10), we next explored the effects of insulin on MARCKS targeting in endothelial cells. We performed confocal fluorescence microscopy and found in resting endothelial cells that MARCKS showed significant staining at the cell border as well as in punctate intracellular membrane-limited structures (Fig. 3*A*). This pattern is strikingly similar to that of the scaffolding/regulatory pro-

tein caveolin-1 (28), which is also robustly expressed in these cells (33). Indeed, as shown in Fig. 3, the pattern of caveolin-1 and MARCKS staining showed significant colocalization in resting endothelial cells. However, within 15 min of adding insulin (100 nM), the pattern of MARCKS staining changed dramatically, as the proportion of MARCKS that colocalized with caveolin plummeted from ~70 to ~10% ($p < 0.001$). Fig. 3*A* shows representative photomicrographs of fixed endothelial cells stained for MARCKS and caveolin-1. Fig. 3*B* shows a quantitative analysis of data pooled from five independent experiments, which documented a significant translocation of MARCKS from peripheral membrane structures to intracellular membrane-limited structures after exposure to insulin.

This striking change in MARCKS localization following insulin exposure prompted us to study some of the known MARCKS binding partners that also have a distinct subcellular distribution. The phospholipid PIP_2, which binds to MARCKS (8) and is localized in both caveolar as well as noncaveolar membrane fractions (27), has been implicated in insulin signaling (4, 28, 34, 35). We therefore pursued several interdependent lines of investigation to explore the role of MARCKS in PIP_2 distribution in resting and insulin-treated endothelial cells. We used an extensively validated hydrodynamic method that uses discontinuous sucrose density gradients to resolve caveolae/lipid rafts from other cellular constituents, and we found that MARCKS was present in both caveolar and noncaveolar fractions. We assayed these same fractions for PIP_2 using a PIP_2-specific fusion protein that permits detection of PIP_2 by immunochemical methods (27). Fig. 4*A* shows a representative blot, and Fig. 4*B* shows pooled data from six independent experiments. Following insulin treatment, there was an ~2-fold increase in the amount of PIP_2 in lipid raft/caveolar fractions; the insulin response was blocked by the PI3K inhibitor LY294002. We were intrigued to observe that siRNA-mediated MARCKS knockdown markedly suppressed the basal level of PIP_2 in caveolar fractions (Fig. 4). As also shown in Fig. 4, MARCKS knockdown attenuated but did not completely block the insulin-promoted increase in PIP_2 seen in control siRNA-transfected cells. We complemented these biochemical approaches by using cell imaging methods with PIP_2-sensitive biosensors (Fig. 5). We utilized a highly specific and well characterized FRET biosensor (20) that permits imaging and quantitation of PIP_2, which can be detected as a FRET signal when PIP_2 promotes the interaction of PLCδ1-YFP and PLCδ1-CFP constructs. We transfected endothelial cells with these PIP_2 biosensors, along with either control or MARCKS siRNA. Fig. 5*A* shows representative live-cell FRET images of endothelial cells, revealing PIP_2 at the external membrane of endothelial cells. Insulin treatment led to a significant increase in FRET, which could be abolished by siRNA-mediated MARCKS knockdown; Fig. 5*B* shows quantitative analyses of pooled data that document a near-total abrogation of the PIP_2-derived FRET signal following MARCKS knockdown.

In addition to PIP_2, other major binding partners of MARCKS include actin and actin-binding proteins (10). We therefore analyzed the effects of siRNA-mediated MARCKS knockdown on the actin cytoskeleton. As shown in Fig. 6,

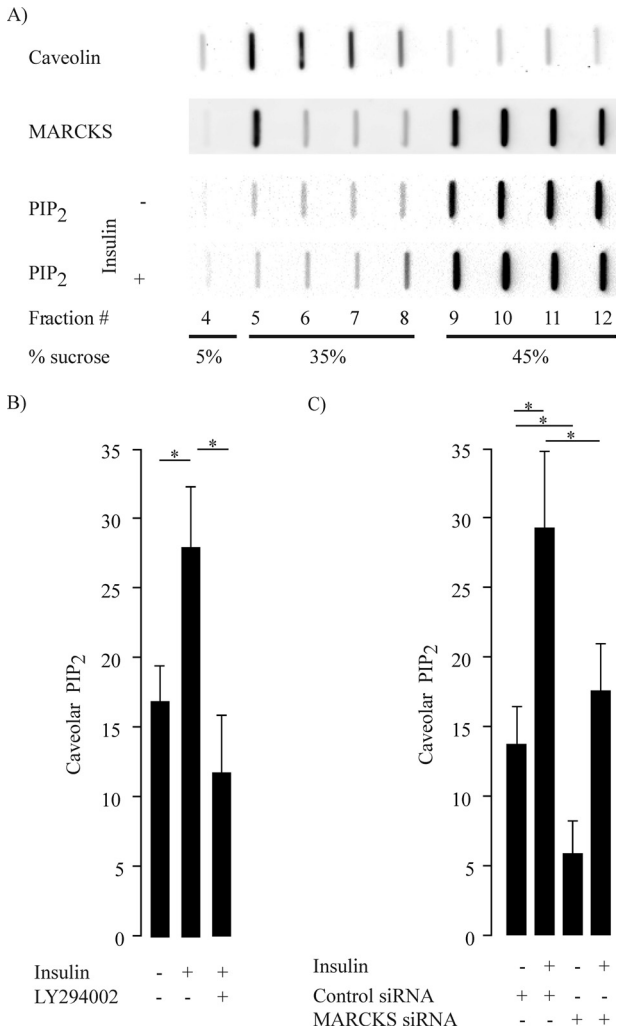

FIGURE 4. **Hydrodynamic analysis of MARCKS, caveolin-1, and PIP_2 distribution in endothelial cells.** *A*, the results of subcellular fractionation of endothelial cells analyzed in discontinuous sucrose gradients to resolve lipid rafts/caveolae (fractions 5–8) and nonlipid raft cellular constituents (fractions 9–12). Aliquots of each fraction were analyzed in slot blots that were probed with specific antibodies directed against MARCKS, caveolin-1, or PIP_2, as shown. PIP_2 distribution was also analyzed following insulin treatment of endothelial cells (100 nM for 15 min). *B*, quantitative analyses of PIP_2 in the lipid raft/caveolar fraction following treatments of endothelial cells with insulin (100 nM for 15 min). PIP_2 content was quantitated by densitometric analysis of slot blots probed with antibodies directed against phospholipid-specific PH domains, and the amount of PIP_2 in the lipid raft fraction was normalized to the total amount of PIP_2 in all fractions. The data are expressed as a percentage of the amount of PIP_2 detected in the lipid raft fraction. The graph on the *left* shows quantitation of PIP_2 in caveolar fractions following insulin treatment in the presence or absence of the PI3K inhibitor LY294002 (10 mM). The graph on the *right* shows the distribution of PIP_2 in caveolar fractions in endothelial cells transfected with control siRNA or siRNA directed against MARCKS. *, $p < 0.01$ compared with control siRNA-transfected cells ($n = 6$).

MARCKS knockdown led to a marked derangement of the actin cytoskeleton compared with control siRNA-transfected cells stained with phalloidin/Alexa Fluor 568. VEGF treatment of control siRNA-transfected endothelial cells promoted a marked increase in stress fiber former, whereas insulin led to an increase in cortical actin. For both the VEGF- and insulin-treated cells, siRNA-mediated MARCKS knockdown led to a striking derangement in cellular actin organization (Fig. 6).

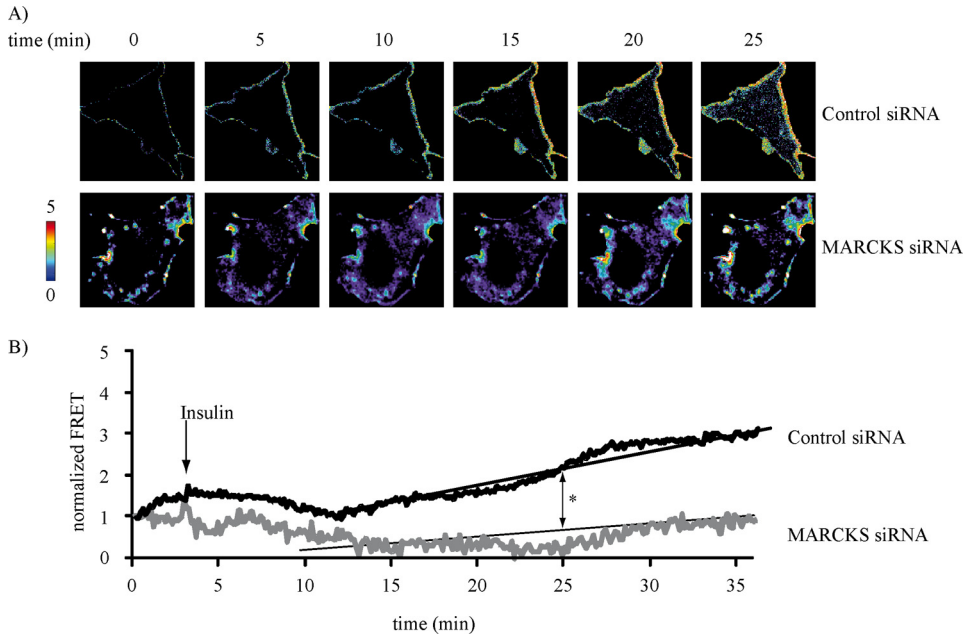

FIGURE 5. **FRET-based analysis of insulin-stimulated PIP_2 accumulation following siRNA-mediated MARCKS knockdown.** *A*, representative images of endothelial cells transfected with PIP_2 biosensor plasmids plus either control or MARCKS siRNA constructs; the individual panels show the time lapse of FRET images obtained following treatment with insulin (100 nM) or vehicle at the indicated times. *B*, pooled quantitative data from six independent experiments. The data are expressed as change of FRET ratio over time, reflecting the abundance of PIP_2 at the plasma membrane. *, $p < 0.01$ ($n = 6$), as compared with control treated cells.

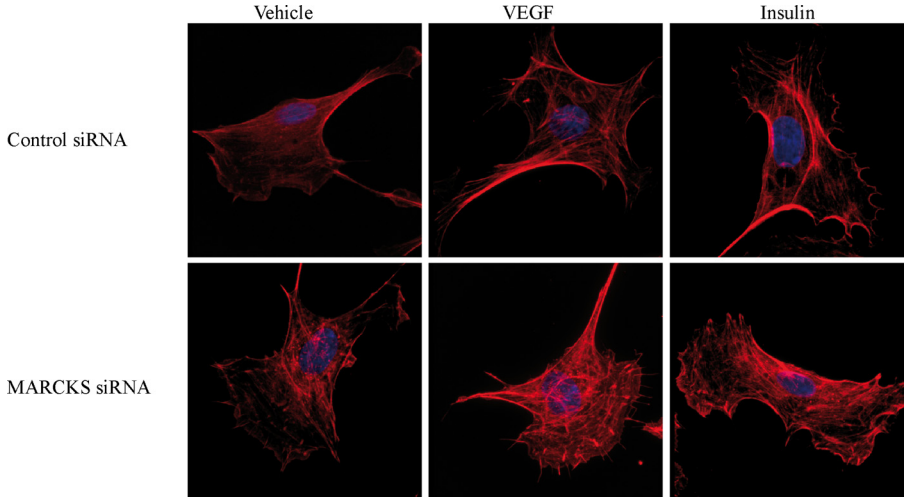

FIGURE 6. **Effects of siRNA-mediated MARCKS knockdown on the endothelial cell actin cytoskeleton.** Shown are representative photomicrographs obtained in endothelial cells that were transfected with control or MARCKS siRNA, treated for 30 min with vehicle, VEGF (20 ng/ml), or insulin (100 nM) as shown, and then fixed and stained with phalloidin/Alexa Fluor 568 using the manufacturer's protocols. Fluorescent micrographic images were analyzed at $\lambda = 573$ nM using an Olympus DSU confocal imaging system (magnification ×100).

Given our results showing that insulin modulates MARCKS-PIP_2 dynamics (Figs. 4 and 5), as well as our observation that MARCKS knockdown disrupts the actin cytoskeleton (Fig. 6), we decided to study two actin-binding proteins that are also involved in PIP_2 pathways, N-WASP and Arp2/3 (12, 14, 36). As shown in Fig. 7, insulin promoted an ~4-fold increase in the phosphorylation of N-WASP at Tyr-256 and Ser-484 and led to a similar increase in Arp2/3 phosphorylation at Tyr-237. The extent of insulin-stimulated N-WASP and Arp2/3 phosphorylation was markedly reduced by siRNA-mediated MARCKS knockdown, as shown in Fig. 7 (a $p < 0.05$ or $p < 0.01$ decrease in phosphorylation following MARCKS knockdown compared with control siRNA-transfected cells, as indicated; $n = 4$). We complemented these immunoblot analyses with cell imaging approaches using a FRET-based N-WASP biosensor that has been extensively validated as a marker for N-WASP/Arp2/3 activation, in which the activation of N-WASP leads to a decrease in the FRET signal from this biosensor (21). Insulin treatment of control siRNA-transfected endothelial cells promoted a significant ~80% decrease in FRET, consistent with N-WASP activation (Fig. 8). Following siRNA-mediated MARCKS knockdown, insulin-promoted N-WASP activation was significantly attenuated ($p < 0.01$, $n = 6$), as shown in the representative time-lapse images (Fig. 8*A*) and quantitated in the analysis of pooled data (Fig. 8*B*).

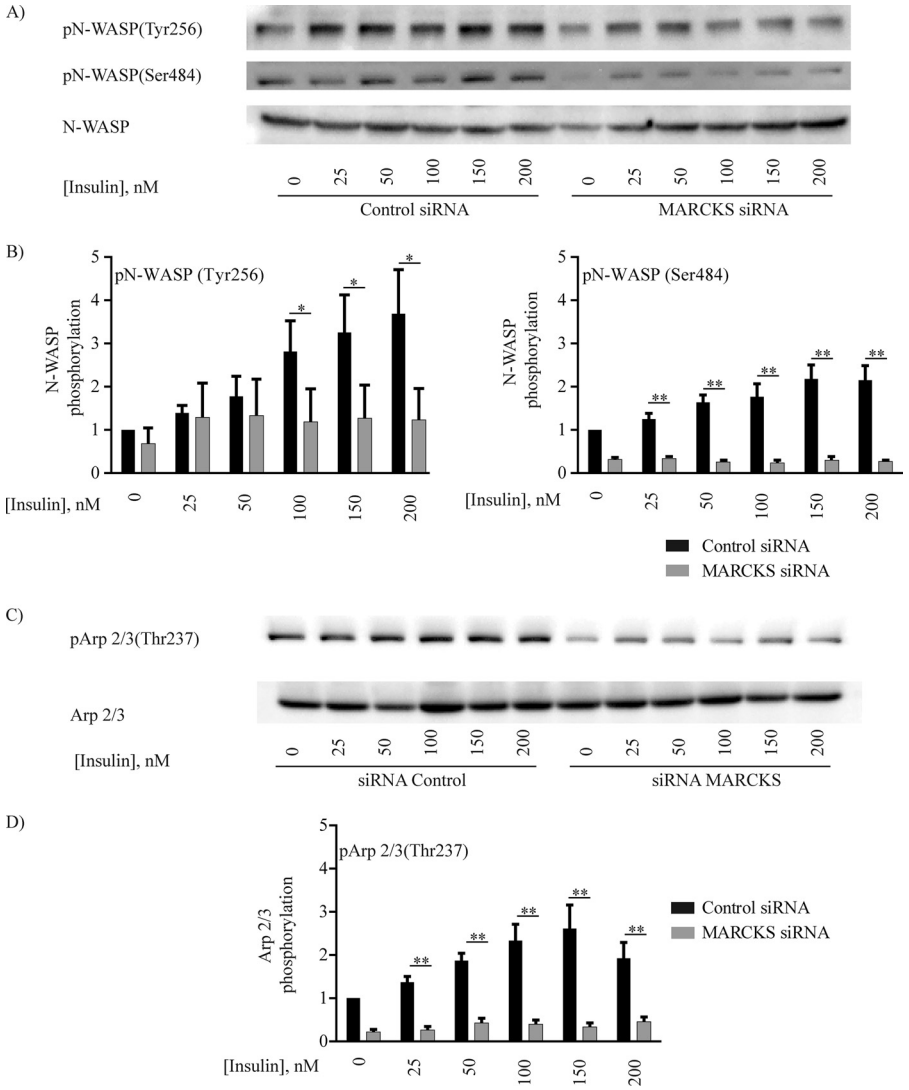

FIGURE 7. **Insulin-promoted phosphorylation of N-WASP and Arp2/3 in cultured endothelial cells.** Show are immunoblots from an insulin dose-response experiment probed with antibodies directed against the PIP$_2$- and actin-binding proteins N-WASP (*A* and *B*) and Arp2/3 (*C* and *D*). Lysates prepared from insulin-treated BAEC were resolved by SDS-PAGE and analyzed in immunoblots probed with antibodies for total or phospho-N-WASP (phosphorylated residues pTyr-256 (*pN-WASP(Tyr256*) and pSer-484 (*pN-WASP(Ser484*), as shown) or total or phospho-Arp2/3 (pTyr-265). *A* and *C*, representative immunoblots. *B* and *D*, quantitative plots derived from pooled data. Each bar in the graphs represents the mean ± S.E. of four independent experiments that yielded similar results. *, $p < 0.05$; **, $p < 0.01$.

DISCUSSION

MARCKS has been extensively characterized as a PIP$_2$- and actin-binding phosphoprotein in many cell types (1, 2, 8–11), but the roles of MARCKS in endothelial cell responses have been almost entirely unexplored before this study. Both the actin cytoskeleton and intracellular PIP$_2$ pathways have been extensively implicated in control of cell motility and migration (4–6, 12, 36). The known characteristics of MARCKS as an actin- and PIP$_2$-binding protein led us to perform experiments investigating the effects MARCKS on endothelial cell migration. We used the scratch wound assay, which has been extensively characterized as a method to analyze directional migration in endothelial cells (29, 37, 38). Control siRNA-treated endothelial cells rapidly and completely fill the gap left after inducing a scratch wound in the endothelial monolayer. By contrast, siRNA-mediated MARCKS knockdown markedly attenuates the directional migration of cells into the scratch wound and also completely blocks VEGF-induced directional migration. These findings in endothelial cells are consistent with recent reports (2, 11) that described a prominent role for MARCKS in the control of axon guidance in neurons. Clearly, MARCKS plays a critical role in the directional migration of endothelial cells, and we sought to explore the more proximal intracellular pathways that are influenced by MARCKS.

Numerous previous studies have examined the effects of insulin on phosphorylation of endothelial signaling proteins, and we chose to examine the effects of insulin on MARCKS-modulated pathways in these cells. We found that insulin-dependent phosphorylation of MARCKS parallels the pattern seen for insulin-dependent phosphorylation of the kinase Akt. Insulin promotes a robust and sustained phosphorylation of Akt and MARCKS for both phosphoproteins, each protein being phosphorylated at an insulin concentration frequently

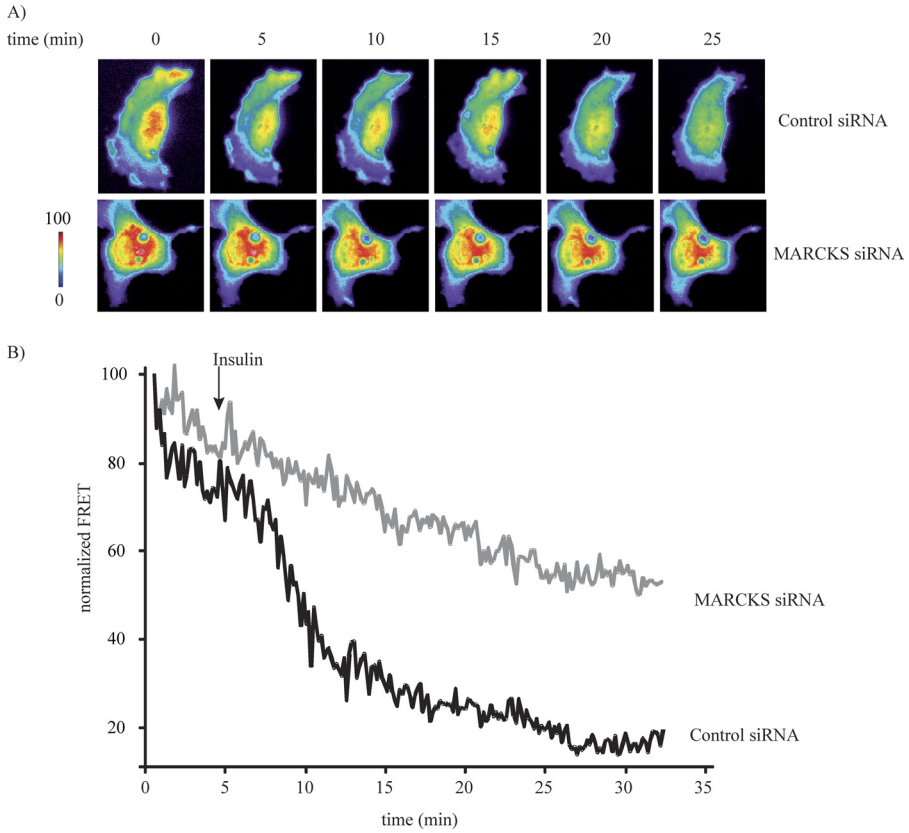

FIGURE 8. **Analysis of N-WASP activation using a FRET based N-WASP biosensor after siRNA-mediated MARCKS knockdown.** *A*, representative images of endothelial cells transfected with the N-WASP FRET biosensor plasmid plus either control or MARCKS siRNA constructs. Following addition of insulin, cells were monitored for the appearance of YFP emission after CFP excitation; the individual panels show the time lapse of FRET images obtained following treatment with insulin (100 nM) or vehicle at the indicated times. Parameter correction was carried out with the MetaMorph FRET module. *B*, pooled quantitative data from six independent experiments. The data are expressed as the change of FRET ratio over time, which reflects the degree of N-WASP activation. *, $p < 0.01$ ($n = 6$), as compared with control siRNA-transfected cells.

used for analyses of signaling responses in cultured cell systems (33, 34, 39). Insulin-dependent phosphorylation of kinase Akt has been extensively characterized in endothelial cells (32), whereas little is known about insulin signaling to MARCKS. We therefore studied the effects of insulin on MARCKS subcellular localization. Previous reports have identified the presence of MARCKS in plasmalemmal caveolae and/or lipid rafts (4, 6, 27, 28, 40), but there has been little information on the dynamic relationships between MARCKS and caveolin. Our cell imaging studies show that MARCKS colocalizes with the scaffolding/regulatory protein caveolin-1 in resting endothelial cells. However, insulin treatment of endothelial cells causes a major change in the subcellular localization of MARCKS, so the spatial overlap between MARCKS and caveolin-1 virtually disappears within a few minutes of exposure to insulin. We do not mean to infer from the overlap of the MARCKS and caveolin-1 signals that these two proteins directly or even indirectly associate with one another, but it is clear that MARCKS subcellular localization is dynamically and dramatically regulated by insulin.

In addition to targeting key signaling proteins to caveolae, plasmalemmal caveolae also serve as sites for the sequestration of specific signaling lipids, including PIP_2 (5, 28). Using hydrodynamic approaches (26), our studies show that insulin treatment of endothelial cells leads to a significant increase of PIP_2 in the lipid raft fraction. siRNA-mediated MARCKS knockdown significantly reduced the PIP_2 content in lipid rafts and blocked the insulin-promoted increase in caveolar PIP_2 seen in cells transfected with control siRNA. We complemented hydrodynamic approaches by exploiting biosensors to measure PIP_2 using imaging methods developed by Jalink and co-workers (20). We studied endothelial cells transfected with the PIP_2 biosensor and found that siRNA-mediated MARCKS knockdown abrogates the insulin-mediated increase in PIP_2 seen in control siRNA-transfected cells. Taken together, our observations indicate that MARCKS is a critical determinant of insulin-modulated PIP_2 responses in these cells.

We sought to identify intracellular signaling pathways that may serve to integrate the dual roles of MARCKS in its ability to bind both to PIP_2 and to the cytoskeleton. siRNA-mediated MARCKS knockdown leads to the derangement of the endothelial cytoskeleton (Fig. 6). The insulin- or VEGF-induced alterations in the actin cytoskeleton were entirely blocked by MARCKS knockdown. Our experiments have implicated the WAVE protein N-WASP and its actin-binding partner Arp2/3. Insulin promotes the phosphorylation of N-WASP both on Try-256 and Ser-484; phosphorylation on these residues leads to N-WASP activation (14, 18, 19, 36). However, siRNA-mediated MARCKS knockdown markedly suppresses insulin-dependent N-WASP phosphorylation of both of these sites, suggesting that MARCKS plays a key role upstream of

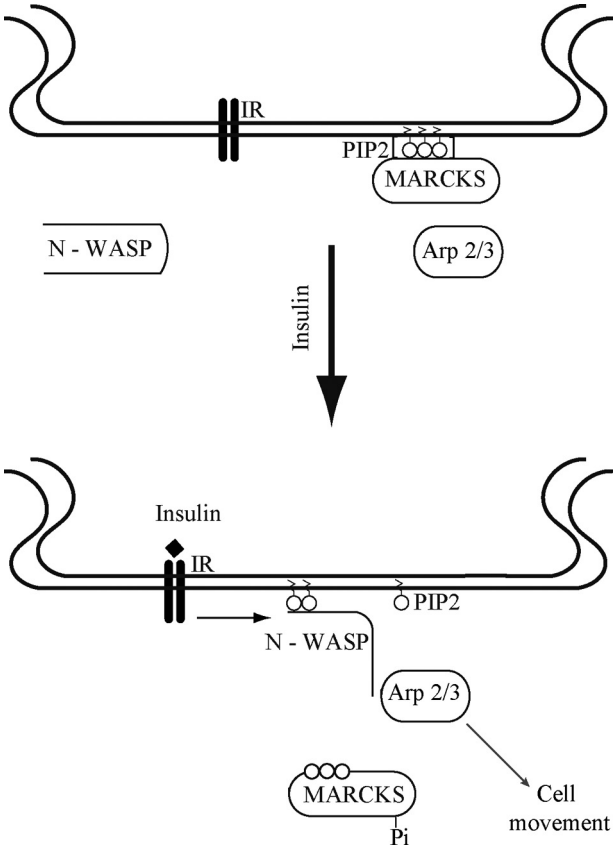

FIGURE 9. **Model for the role of MARCKS in insulin-modulated PIP_2 mobilization.** Shown is a model that integrates the findings in this study that have explored the pathways of insulin-mediated PIP_2 mobilization. In resting endothelial cells (*upper panel*), MARCKS sequesters PIP_2 in caveolae, and N-WASP and Arp2/3 are quiescent and not interacting with one another. Insulin receptor activation (*lower panel*) leads to the mobilization of PIP_2 from MARCKS, accompanied by MARCKS phosphorylation and translocation from caveolae to intracellular sites. The mobilized PIP_2 binds to and activates N-WASP and Arp2/3, leading to alterations in the actin cytoskeleton that are critical determinants of directed endothelial cell movement. See text for further discussion.

N-WASP activation. As might be expected from the known requirement for N-WASP phosphorylation to allow subsequent phosphorylation of Arp2/3 (36), siRNA-mediated MARCKS knockdown was found to a similar inhibitory effect on insulin-promoted Arp2/3 phosphorylation. We extended these biochemical approaches using an N-WASP FRET biosensor (21). Just as we found for N-WASP phosphorylation, siRNA-mediated MARCKS knockdown blocks insulin-dependent activation of the N-WASP biosensor. These independent experimental approaches help to establish a key role for MARCKS in N-WASP/Arp2/3 signaling in endothelial cells.

These observations have helped to expand the regulatory repertoire of MARCKS and to affirm its broad role in endothelial cell signaling. Fig. 9 presents a model that integrates our new experimental findings in the context of previous studies of PIP_2 metabolism and actin polymerization. In resting endothelial cells, MARCKS sequesters PIP_2 in lipid rafts (Figs. 4 and 5) (4, 5, 28, 35). As shown in the schematic in Fig. 9, following insulin-mediated MARCKS phosphorylation (Fig. 2), the protein translocates (Fig. 3), and the PIP_2 thereby released (Figs. 4 and 5) is able to bind to N-WASP and promote its phosphorylation and interaction with Arp2/3 (Figs. 7 and 8). Arp2/3-dependent actin polymerization and remodeling of the cytoskeleton are required for directional cell migration (Fig. 1) (13, 41).

These studies document an important relationship between MARCKS and N-WASP in endothelial cells and provide evidence indicating that the PIP_2 required for N-WASP activation is exclusively supplied by MARCKS. These studies establish a role for MARCKS in insulin signaling to PIP_2 and to regulatory proteins in the actin cytoskeleton of vascular endothelial cells. The spectrum of cellular elements interacting with MARCKS spans from the plasmalemmal caveolae to the actin cytoskeleton, with PIP_2 providing a key link between the cell membrane and cytoskeleton that is critically modulated by MARCKS in response to receptor activation. Given the protean role of MARCKS in endothelial cells, it seems plausible that MARCKS may play a role in vascular disease states characterized by deficient endothelium-dependent signaling responses.

Acknowledgments—We thank Dr. Kees Jalink for providing the PIP_2 biosensor, Dr. John Condeelis for the gift of the N-WASP biosensor used in these studies, and Drs. Juliano Sartoretto and Ruqin Kou and other members of the Michel laboratory for helpful discussions.

REFERENCES

1. Larsson, C. (2006) *Cell. Signal.* **18,** 276–284
2. Sheetz, M. P., Sable, J. E., and Döbereiner, H. G. (2006) *Annu. Rev. Biophys. Biomol. Struct.* **35,** 417–434
3. Stumpo, D. J., Bock, C. B., Tuttle, J. S., and Blackshear, P. J. (1995) *Proc. Natl. Acad. Sci. U.S.A.* **92,** 944–948
4. Fujita, A., Cheng, J., Tauchi-Sato, K., Takenawa, T., and Fujimoto, T. (2009) *Proc. Natl. Acad. Sci. U.S.A.* **106,** 9256–9261
5. Anderson, R. G., and Jacobson, K. (2002) *Science* **296,** 1821–1825
6. Gamper, N., and Shapiro, M. S. (2007) *J. Physiol.* **582,** 967–975
7. Stahlhut, M., and van Deurs, B. (2000) *Mol. Biol. Cell* **11,** 325–337
8. Arbuzova, A., Schmitz, A. A., and Vergères, G. (2002) *Biochem. J.* **362,** 1–12
9. Hartwig, J. H., Thelen, M., Rosen, A., Janmey, P. A., Nairn, A. C., and Aderem, A. (1992) *Nature* **356,** 618–622
10. Yarmola, E. G., Edison, A. S., Lenox, R. H., and Bubb, M. R. (2001) *J. Biol. Chem.* **276,** 22351–22358
11. Calabrese, B., and Halpain, S. (2005) *Neuron* **48,** 77–90
12. Papayannopoulos, V., Co, C., Prehoda, K. E., Snapper, S., Taunton, J., and Lim, W. A. (2005) *Mol. Cell* **17,** 181–191
13. Sarmiento, C., Wang, W., Dovas, A., Yamaguchi, H., Sidani, M., El-Sibai, M., Desmarais, V., Holman, H. A., Kitchen, S., Backer, J. M., Alberts, A., and Condeelis, J. (2008) *J. Cell Biol.* **180,** 1245–1260
14. Weisswange, I., Newsome, T. P., Schleich, S., and Way, M. (2009) *Nature* **458,** 87–91
15. Arnold, T. P., Standaert, M. L., Hernandez, H., Watson, J., Mischak, H., Kazanietz, M. G., Zhao, L., Cooper, D. R., and Farese, R. V. (1993) *Biochem. J.* **295,** 155–164
16. Jiang, Z. Y., He, Z., King, B. L., Kuroki, T., Opland, D. M., Suzuma, K., Suzuma, I., Ueki, K., Kulkarni, R. N., Kahn, C. R., and King, G. L. (2003) *J. Biol. Chem.* **278,** 31964–31971
17. Baron, A. D. (2002) *J. Diabetes Complications* **16,** 92–102
18. Wu, X., Suetsugu, S., Cooper, L. A., Takenawa, T., and Guan, J. L. (2004) *J. Biol. Chem.* **279,** 9565–9576
19. Cai, L., Marshall, T. W., Uetrecht, A. C., Schafer, D. A., and Bear, J. E. (2007) *Cell* **128,** 915–929
20. van Rheenen, J., Achame, E. M., Janssen, H., Calafat, J., and Jalink, K. (2005) *EMBO J.* **24,** 1664–1673

21. Lorenz, M., Yamaguchi, H., Wang, Y., Singer, R. H., and Condeelis, J. (2004) *Curr. Biol.* **14,** 697–703
22. Dykxhoorn, D. M., Novina, C. D., and Sharp, P. A. (2003) *Nat. Rev. Mol. Cell Biol.* **4,** 457–467
23. Elbashir, S. M., Harborth, J., Lendeckel, W., Yalcin, A., Weber, K., and Tuschl, T. (2001) *Nature* **411,** 494–498
24. Michel, T., Li, G. K., and Busconi, L. (1993) *Proc. Natl. Acad. Sci. U.S.A.* **90,** 6252–6256
25. Gonzalez, E., Kou, R., and Michel, T. (2006) *J. Biol. Chem.* **281,** 3210–3216
26. Song, K. S., Li, S., Okamoto, T., Quilliam, L. A., Sargiacomo, M., and Lisanti, M. P. (1996) *J. Biol. Chem.* **271,** 9690–9697
27. Yamaguchi, H., Shiraishi, M., Fukami, K., Tanabe, A., Ikeda-Matsuo, Y., Naito, Y., and Sasaki, Y. (2009) *J. Cell. Physiol.* **220,** 748–755
28. Watt, S. A., Kular, G., Fleming, I. N., Downes, C. P., and Lucocq, J. M. (2002) *Biochem. J.* **363,** 657–666
29. Soderholm, J., and Heald, R. (2005) *Chem. Biol.* **12,** 263–265
30. Jin Cho, S., La, M., Ahn, J. K., Meadows, G. G., and Joe, C. O. (2001) *Biochem. Biophys. Res. Commun.* **283,** 273–277
31. Robinson, P. J., Liu, J. P., Chen, W., and Wenzel, T. (1993) *Anal. Biochem.* **210,** 172–178
32. Zeng, G., Nystrom, F. H., Ravichandran, L. V., Cong, L. N., Kirby, M., Mostowski, H., and Quon, M. J. (2000) *Circulation* **101,** 1539–1545
33. Gonzalez, E., Nagiel, A., Lin, A. J., Golan, D. E., and Michel, T. (2004) *J. Biol. Chem.* **279,** 40659–40669
34. Saltiel, A. R., and Pessin, J. E. (2003) *Traffic* **4,** 711–716
35. Schwencke, C., Braun-Dullaeus, R. C., Wunderlich, C., and Strasser, R. H. (2006) *Cardiovasc. Res.* **70,** 42–49
36. Prehoda, K. E., Scott, J. A., Mullins, R. D., and Lim, W. A. (2000) *Science* **290,** 801–806
37. Liang, C. C., Park, A. Y., and Guan, J. L. (2007) *Nat. Protoc.* **2,** 329–333
38. Yarrow, J. C., Perlman, Z. E., Westwood, N. J., and Mitchison, T. J. (2004) *BMC Biotechnol.* **4,** 21
39. Yamagishi, S. I., Edelstein, D., Du, X. L., Kaneda, Y., Guzmán, M., and Brownlee, M. (2001) *J. Biol. Chem.* **276,** 25096–25100
40. Lajoie, P., Goetz, J. G., Dennis, J. W., and Nabi, I. R. (2009) *J. Cell Biol.* **185,** 381–385
41. Baba, Y., Nonoyama, S., Matsushita, M., Yamadori, T., Hashimoto, S., Imai, K., Arai, S., Kunikata, T., Kurimoto, M., Kurosaki, T., Ochs, H. D., Yata, J., Kishimoto, T., and Tsukada, S. (1999) *Blood* **93,** 2003–2012